TDR 2006
Purdue University

Improvements of Spatial-TDR for Hydrological and Geotechnical Applications

Stefan Schlaeger, Rolf Becker, Wolfram Schadel, Alexander Scheuermann, Holger Worsching

Ref.: Schlaeger, Stefan, Becker, Rolf, Schadel, Wolfram, Scheuermann, Alexander and Worsching, Holger, "Improvements of Spatial-TDR for Hydrological and Geotechnical Applications", Proc. TDR 2006, Purdue University, West Lafayette, USA, Sept. 2006, Paper ID 31, 19 p., https://engineering.purdue.edu/TDR/Papers

Improvements of Spatial-TDR
for Hydrological and Geotechnical Applications

Stefan Schlaeger[1,2], Rolf Becker[1,3,4], Wolfram Schädel[1,3],
Alexander Scheuermann[1,5], Holger Wörsching [1,5]

[1] Soil Moisture Group (SMG), University of Karlsruhe, Germany
[2] SCHLAEGER – mathematical solutions & engineering, Horn-Bad Meinberg, Germany
[3] Institute for Water and River Basin Management, University of Karlsruhe, Germany
[4] IMKO – Micromodultechnik, Ettlingen, Germany
[5] Institute of Soil Mechanics and Rock Mechanics, University of Karlsruhe, Germany

Abstract

The spatial distribution of soil moisture in the vadose zone and its evolution in time gives valuable information to many applications in hydrology, soil science or geotechnics. The Soil Moisture Group has developed and established an inversion technique to derive moisture profiles along single TDR sensor-probes from 0,40 to 5,00 meters. The algorithm uses the full information content of TDR reflection data measured from one or both sides of an embedded probe. The system consisting of sensor-probe and surrounded soil can be interpreted as a nonuniform transmission-line. The algorithm is based on the telegraph equations for nonuniform transmission-lines and an optimization approach to reconstruct the distribution of the capacitance and effective conductance along the transmission-line with high spatial resolution. The capacitance distribution can be converted into permittivity and water content by means of a capacitance model and dielectric mixing rules. Single- and double-sided time-domain reflection data were used to determine the capacitance and effective conductance profiles of low-loss and lossy soils. The results show that single-sided reflection data are sufficient for the low-loss material. This can be extended to lossy material correlating capacitance and conductance. If this correlation is not available, two independent reflection measurements are required to reconstruct a reliable soil moisture profile. The inclusion of an additional effective conductivity profile leads to an improved capacitance profile. The algorithm converges very fast and yields a capacitance profile within a sufficiently short time. The additional transformation to the water content requires no significant calculation time.
Single- and double-sided sensor-probes have been analyzed. Experimental results obtained in various projects dealing with measurements and monitoring of water content (water transport processes in a full scale levee model or flood warning systems in small catchment areas) demonstrate the applicability of the proposed methods for practical problems.

Key Words: Soil moisture, inversion technique, transient hydraulic processes, flood warning

Introduction

The water content of soils and other porous materials is one of the most important parameters in hydrology, agriculture and civil engineering. Standard methods such as oven-drying are very time-consuming and destructive, neutron moderation or gamma attenuation measurements make use of critical radioactive sources. The determination of moisture content with time-domain reflectometry (TDR) technology is based on measurements of travel-time of an electromagnetic pulse on a transmission-line of known length. A review about TDR techniques for the measurement of permittivity and bulk electrical conductivity, but also for probe design and probe construction is given in Robinson et al., 2003[1]. For homogeneous materials the travel-time is directly related to the permittivity, which is in common porous materials mainly a function of water content (Brichak et al., 1974[2]; Topp et al., 1980[3], 1982[4][5]; Topp and Davis 1985[6]; Dasberg and Dalton 1985[7]).

One type of TDR transmission-line commonly used in many soil moisture relevant applications is an unshielded metallic fork, which is inserted into the material under test. The maximum length is limited, because the electromagnetic pulse is attenuated and disappears on longer lines. For longer transmission-line sensors insulated probes are more capable. The use of automation and multiplexing capability (i.e. Heimovaara and Bouten, 1990[8]) increases the ability to monitor the dynamics and spatial distribution of water content.
So far TDR technology using single probes was limited to an integral or very coarsely resolved water content determination along the sensor line. But many applications ask for the spatial moisture distribution in soils or building constructions along a given profile. Different approaches have been developed to use TDR information for the determination of soil moisture profiles (multisection transmission lines: Hook et al., 1992[9]; Feng et al., 1999[10]; full wave inversion techniques: Pereira, 1997[11]; Todoroff et al, 1998[12]; Oswald, 2000[13]; Heimovaara et al. 2004[14]). A high spatial resolution can be achieved by exploiting the full information content in the reflected electromagnetic signals of the sensor line (Lundstedt and He, 1996[15]; Norgren and He, 1996[16]). A new reconstruction algorithm has been developed which uses the full information of the TDR signals measured on one or both sides of the line. It is based on the telegraph equation for nonuniform transmission-lines and an optimization approach to reconstruct simultaneously one or two line parameters with high spatial resolution (Schlaeger, 2002[17], 2005[18]). In comparison with other full wave inversion techniques (e.g. generic algorithms, Oswald, 2000[13]) it needs clearly less computation expenditure. The optimization algorithm uses the conjugate-gradient-technique and fast simplex or complex methods.
Using laboratory tests it is shown that TDR reflection data from both sides of a buried flat-ribbon-cable sensor are suitable for simultaneous reconstruction of capacitance and effective conductance profiles. During an investigation of the transport of volatile organic compounds in medium grained sand (grain size 0.2 to 1 mm) the moisture profile under irrigation has been measured. In the steady state the volumetric water content varies along the vertically arranged transmission-line sensor of 71.7 cm between 0.5 and 44 %. The changes in water content could be reconstructed with a high spatial accuracy and an average uncertainty of ±2.3 % compared to oven-drying measurements[1].

To determine moisture profiles, appropriate TDR-devices (short pulse rise time, high sampling rate) and sensitive testing probes (well known electric parameters) are required. The mathematical model has to be chosen to describe the physical process during the measurement in a very accurate and computable way. The inversion algorithm starts with an initial guess of the electric parameter distribution. Using this parameter distribution an associated TDR-signal can be calculated. The difference between the measurement and this simulation leads to a rough deformation-instruction for the given parameter distribution. During one optimization-step a new parameter distribution will be generated by deforming the old distribution according to the deformation-instruction. In the next step the comparison between measurement and simulation

---

[1] Schlaeger, S., C. Hübner, and K. Weber, Moisture profile determination with TDR, in preparation.

leads to an improved deformation-instruction. The optimization will be continued until a minimum difference is reached. The resulting electric parameter distribution can be easily transformed into water content profiles. The whole process is called Spatial-TDR.

The Soil Moisture Group (SMG) at the University of Karlsruhe has tested this Spatial-TDR technology in many applications. A monitoring system to measure the spatial soil water distribution on a full-scale levee model has been successfully implemented with transmission-lines up to 3 m and leads to significant specifications for drainage models (Scheuermann et al., 2001[19]). The technology is also being used for flood warning systems, and snow moisture measurements (Becker et al., 2002[20]; Stacheder et al., 2005[21]), and for the determination of the water content of technical barriers in waste disposal sites (Becker et al., 2003[22]).

Basic equations

The propagation of electromagnetic waves on insulated and non insulated transmission-lines can be described by the telegraph equations. These equations were developed by Heaviside in 1886. In this model the transmission-line is characterized by four electrical parameters: the inductance *L*, capacitance *C*, series resistance *R*, and shunt conductance *G*. The equivalent electric circuit of an infinitesimal transmission-line section is given in Figure 1. It is seen that the inductance and resistance are series elements that cause a voltage drop along the line, whereas the capacitance and conductance are shunt elements that provide a current path between the conductors.

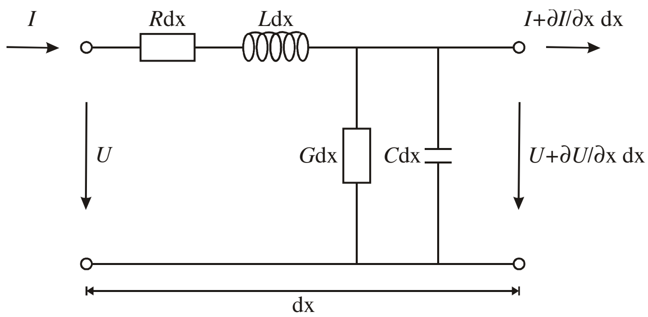

Fig.1. Equivalent circuit of an infinitesimal section of a transverse electromagnetic (TEM) transmission-line

From a circuit theory approach it is a simple matter to derive the telegraph equations that describe the variation of the voltage *U(x,t)* and the current *I(x,t)* in the time along the transmission-line due to the influence of the electric parameters of the line and the surrounding media. By applying Kirchhoff's voltage and current laws to the equivalent circuit in Figure 1, one obtains

$$\frac{\partial}{\partial x}U(x,t) = -R(x)I(x,t) - L(x)\frac{\partial}{\partial t}I(x,t), \tag{1}$$

$$\frac{\partial}{\partial x}I(x,t) = -G(x)U(x,t) - C(x)\frac{\partial}{\partial t}U(x,t). \tag{2}$$

Usually *R* and *L* are constant for the probe whereas *C* and *G* depend on the surrounding material. In most cases *R* can be neglected. The conductance *G* of transmission-line sensors embedded in soil depends on soil type, water content, and frequency. Usually clayey and loamy soils have much higher conductivity than sands. The capacitance *C* is intimately connected with the permittivity and therefore the water content of the surrounding medium. The determination of the spatial distribution of $C(x)$ is the key component of the presented reconstruction of the soil water content.

The solution of (1) and (2) describes the propagation in time and space of a supplied pulse to the whole measurement system. When the solution is restricted to one spatial point it represents a simulated measurement in this point. To calculate the solution initial and boundary conditions for the partial differential equations (PDE) are needed. It is also important to consider the connection between TDR-device and testing probe. Usually they are connected with a lossless and uniform coaxial-cable (R=0, G=0, C=const, and L=const). Assume that there is no energy on the line at the beginning of the measurement. So the initial conditions can be set to

$$U(x,t)_{t\le 0}=0,\;\; I(x,t)_{t\le 0}=0,\;\text{for all } x. \tag{3}$$

Than the equations (1) and (2) can be transformed to one single PDE of second order

$$\left[LC\frac{\partial^2}{\partial t^2}+LG\frac{\partial}{\partial t}+\frac{\partial L/\partial x}{L}\frac{\partial}{\partial x}-\frac{\partial^2}{\partial x^2}\right]U(x,t)=0. \tag{4}$$

The derivative of L has to be considered in (4) because the inductance of the coaxial-cable and the testing probe are constant but may be different in general. The initial conditions (3) can be transformed to

$$U(x,t)\big|_{t\le 0}=0,\;\;\frac{\partial}{\partial t}U(x,t)\big|_{t\le 0}=0,\;\text{for all } x. \tag{5}$$

To define the boundary conditions for the PDE (4) the whole measurement configuration has to be considered. The sensitive transmission-line has to be inserted into the soil and must be connected to a TDR-device in order to excite an electric pulse.

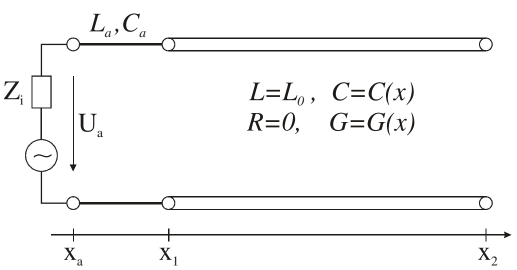

Fig.2. Schematic representation of a sensitive transmission-line, situated between x_1 and x_2, which is connected to a TDR-device on one side using a lossless uniform coaxial-cable with impedance $Z=(L_a/C_a)^{0.5}$

Figure 2 describes the experimental setup to receive the reflection data from one side of the sensitive transmission-line. Therefore reflection measurements must be realized with an external current $F_{ex}=\delta(x-x_a)\cdot f(t)$ at $x=x_a$. The back-traveling wave is absorbed by the matched impedance Z_i inside the TDR-device if it is equal to the impedance Z of the coaxial-cable. This absorbing boundary condition for the lossless wave equation can be numerically implemented in the coaxial-cable using (Engquist and Majda, 1977[23]:

$$\left[\frac{\partial}{\partial x} - \sqrt{L_a C_a}\frac{\partial}{\partial t}\right] U(x_a, t) = L_a \frac{\partial}{\partial t} F_{ex}(x_a, t), \qquad t \geq 0. \tag{6}$$

The boundary conditions at the end of the sensitive line at $x=x_2$ depends on its physical implementation. In case of an open-circuit the boundary condition will be

$$\frac{\partial}{\partial t} U(x_2, t) = 0, \qquad t \geq 0. \tag{7}$$

If there is a short-circuit at $x=x_2$ the boundary condition will be $U(x_2,t) = 0$, for $t \geq 0$.

In order to reconstruct two parameters, two independent measurements are needed. Consequently, the problem is divided into two parts, the first dealing with an incident wave from the left and the second with an incident wave from the right side of the system under test.

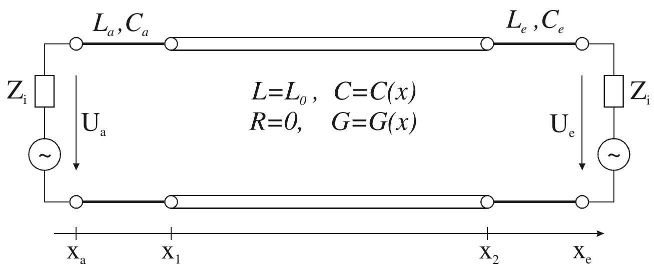

Fig. 3. The nonuniform transmission-line, situated between x_1 and x_2, is connected to two lossless uniform coaxial-cables with matched impedances Z_i at their endpoints

Figure 3 describes the experimental setup to receive the reflection data from both sides of the unknown material. Therefore two separate measurements must be realized with the external current $F^1_{ex}=\delta(x-x_a)\cdot f(t)$ and $F^2_{ex}=\delta(x-x_e)\cdot f(t)$, respectively. $U_1(x,t)$ and $U_2(x,t)$ are the solutions of both separate forward problems. The setup of Figure 3 can be transformed to the setup in Figure 2 for each single-sided measurement using sensor switches (Becker and Hübner, 2003[24]). In this case the solution of $U_1(x,t)$ can be calculated according to $U(x,t)$ by using (4)-(7). If there is a coaxial-cable permanently attached at $x=x_e$ an absorbing boundary condition has to be used instead of (7):

$$\left[\frac{\partial}{\partial x} + \sqrt{L_e C_e}\frac{\partial}{\partial t}\right] U_1(x_e, t) = 0, \qquad t \geq 0 \tag{8}$$

For the other initial-boundary-value-problem (IBVP) for U_2 with external current F^2_{ex} the boundary conditions are exchanged.

Before the reconstruction procedure can be started all necessary parameters (L_a, C_a, L_e, C_e, L_0) have to be measured or calculated (Becker, 2004[25]; Becker and Schlaeger, 2005[26]). The inverse method presented in the next section is based on an iterative search for the electrical parameters of the nonuniform transmission-line with the full wave solution of the direct problem. The solution of the line needs to be calculated repetitively. It is therefore important to use a technique for the determination of this solution that is computationally efficient to guarantee low calculating time.

Optimization approach

The aim of the investigation is the determination of the unknown distribution of *C(x)* with measurements of input and output data. The input data *f(t)*, which describes the incident pulse, can be easily determined from the reflection measurements $U_a(x_a,t)$ of the coaxial-cable between x_a and x_1 with an open-circuit at $x=x_1$. The output data $\lambda(t)$ is the reflected signal based on the associated input signal at one side of the sensor line.
The cost function *J(C)* defines the squared difference (in L_2-norm) between the solution of the direct problem (4)-(7) restricted to $x=x_1$ corresponding to one given parameter distribution *C* and the measured reflections $\lambda(t)$ at $x=x_1$,

$$J(C) = \left\| U(x_1,t;C) - \lambda(t) \right\|_2^2 = \int_0^{2T} \left[U(x_1,t;C) - \lambda(t) \right]^2 dt \tag{9}$$

with $T=\tau(x_1,x_2)$, where $\tau(x_1,x_2)$ is the travel-time between x_1 and x_2. The cost function refers to the error in the solution for single-sided incidence measurements. The concept of the method is to find the parameter distribution that minimize the cost functional *J*. If the problem has a solution the theoretical minimum of *J* is zero. One important reason for choosing the L_2-norm is the possibility to derive exact expressions for the gradient of *J*.

Exact expression of the gradient of the cost function

In the following section the gradient of the cost function will be determined for single-sided and double-sided reflection data, respectively. For one single measurement it is only possible to calculate one parameter distribution *C(x)* or *G(x)* while the other one is known (He et al., 1993[27]). Assuming that the capacitance and conductance are connected by a transfer function then it is possible to calculate both parameter distributions from one single reflection measurement using an empirical *G(C)*-relationship (Hakansson, 1997[28]). This relationship depends not only on the water content but also on the electrolyte imbalance of the pore water. The determination of this relation may be very time intensive (Becker, 2004[25]; Becker and Schlaeger, 2005[26]). If both parameter distributions are to be calculated simultaneously without this *G(C)*-relationship, two independent measurements have to be carried out, e.g. double-sided reflection measurements (He et al., 1994[29]). In the first case the gradient for $J(\alpha)=J(C)$ or $J(\alpha)=J(G)$, in the second case the gradient for $J(\alpha)=J(C,G)$ is calculated. In both cases the gradient $\nabla J(\alpha)$ can be calculated using the standard finite difference formulation for $\delta\alpha \rightarrow 0$:

$$J(\alpha+\delta\alpha) - J(\alpha) = \left\langle \delta\alpha, \nabla J(\alpha) \right\rangle = \int_{-\infty}^{\infty} \delta\alpha(x) \cdot \nabla J(\alpha)(x) dx \tag{10}$$

Single-sided reflection data

In the case of only one single-sided reflection data-set it is reasonable to reconstruct the capacitance profile *C(x)* to determine the water content. Therefore the information about the gradient $\nabla J(C)$ has to be generated. According to (9) equation (10) can be transferred to

$$
\begin{aligned}
&J(C+\delta C)-J(C) \qquad (11)\\
&=\int_0^{2T}\left[U(x_1,t;C+\delta C)-\lambda(t)\right]^2-\left[U(x_1,t;C)-\lambda(t)\right]^2 dt\\
&=\int_0^{2T}U^2(x_1,t;C+\delta C)-U^2(x_1,t;C)\\
&\qquad -2\lambda(t)\left[U(x_1,t;C+\delta C)-U(x_1,t;C)\right]dt\\
&=\int_0^{2T}\underbrace{\left[U(x_1,t;C+\delta C)+U(x_1,t;C)\right]}_{\approx 2U(x_1,t;C)}\cdot\underbrace{\left[U(x_1,t;C+\delta C)-U(x_1,t;C)\right]}_{=:\delta U(x_1,t;C)}\\
&\qquad -2\lambda(t)\cdot\underbrace{\left[U(x_1,t;C+\delta C)-U(x_1,t;C)\right]}_{=:\delta U(x_1,t;C)}dt\\
&\approx\int_0^{2T}2\delta U(x_1,t;C)\cdot\left[U(x_1,t;C)-\lambda(t)\right]dt\\
&=\int_0^{2T}\int_{-\infty}^{\infty}\delta U(x,t;C)\cdot 2\delta(x-x_1)\left[U(x,t;C)-\lambda(t)\right]dx\,dt
\end{aligned}
$$

In equation (11) *δ(x)* represents the Dirac delta-function with $\int\delta(x-x_0)f(x)=f(x_0)$ for all *f*. The difference between two solutions according to a difference between *C* and *C+δC* is defined by *δU(C)=U(C+δC)-U(C)*. For small discrepancies in *C* the difference *δU(C)* is assumed to be also small and *U(C+δC)+U(C)≈2U(C)*. To make further transformations of (11) the advantages of adjoint operators will be used. Therefore a linear operator **L** is defined analog to equation (4):

$$
\mathbf{L}U\equiv\left[LC\frac{\partial^2}{\partial t^2}+LG\frac{\partial}{\partial t}+\frac{\partial L/\partial x}{L}\frac{\partial}{\partial x}-\frac{\partial^2}{\partial x^2}\right]U \qquad (12)
$$

The definition of the adjoint operator $\mathbf{L}^*$ is that he will fulfil the following equation for every *U(x,t)* and *V(x,t)*

$$
(\mathbf{L}U\,|\,V)=(U\,|\,\mathbf{L}^*V) \qquad (13)
$$

using the inner product

$$
(U\,|\,V)=\int_0^{2T}\int_{-\infty}^{\infty}U(x,t)V(x,t)\,dx\,dt. \qquad (14)
$$

Now the PDE for the adjoint operator $\mathbf{L}^*$ has to be determined. The left side of equation (13) can be transformed using (12) and (14). Each of the double-integrals will be transformed to isolate *U(x,t)* using integration by parts in every addend. The auxiliary terms resulting from this isolation must be eliminated now, as the initial and boundary conditions for *V* are appropriate selected. The notation U_t and U_{tt} in the following equation is an abbreviation for the partial differential derivative $\partial U/\partial t$ and $\partial^2 U/\partial t^2$, respectively.

$$
\begin{aligned}
&(\mathbf{L}U \mid V) \qquad (15)\\
&= \int_0^{2T}\int_{-\infty}^{\infty} LCU_{tt}V dxdt + \int_0^{2T}\int_{-\infty}^{\infty} LGU_t V\, dxdt \\
&\quad + \int_0^{2T}\int_{-\infty}^{\infty} \frac{L_x}{L} U_x V dxdt - \int_0^{2T}\int_{-\infty}^{\infty} U_{xx} V dxdt \\
&= \int_{-\infty}^{\infty} LC\left([U_t V]_{t=0}^{t=2T} - [UV_t]_{t=0}^{t=2T} + \int_0^{2T} UV_{tt} dt \right) dx \\
&\quad + \int_{-\infty}^{\infty} LG\left([UV]_{t=0}^{t=2T} - \int_0^{2T} UV_t dt \right) dx \\
&\quad + \int_0^{2T}\left([U \frac{L_x}{L} V]_{x=-\infty}^{x=\infty} - \int_{-\infty}^{\infty} U \left(\frac{L_x}{L}\right)_x V dx - \int_{-\infty}^{\infty} U \frac{L_x}{L} V_x dx \right) dt \\
&\quad - \int_0^{2T}\left([U_x V]_{x=-\infty}^{x=\infty} - [UV_x]_{x=-\infty}^{x=\infty} + \int_{-\infty}^{\infty} UV_{xx} dx \right) dt \\
&\overset{\#1}{=} \int_0^{2T}\int_{-\infty}^{\infty} LCV_{tt} U dxdt - \int_0^{2T}\int_{-\infty}^{\infty} LGV_t U dxdt \\
&\quad - \int_0^{2T}\int_{-\infty}^{\infty} \frac{L_x}{L} V_x U dxdt - \int_0^{2T}\int_{-\infty}^{\infty} V_{xx} U dxdt \\
&\overset{\#2}{=} (U \mid \mathbf{L}^* V)
\end{aligned}
$$

To make sure that transformation #1 in (15) is correct the initial and boundary conditions for *V(x,t)* have to be set as follows

$$V(x,2T) = 0, \quad \frac{\partial}{\partial t} V(x,2T) = 0, \qquad -\infty < x < \infty, \tag{16}$$

$$V(-\infty,t) = 0, \quad \frac{\partial}{\partial t} V(\infty,t) = 0, \qquad 0 \le t \le 2T. \tag{17}$$

The initial condition results to a backward propagation in time from *2T* to zero. When the operator $\mathbf{L}^*$ is defined by

$$\mathbf{L}^* V \equiv \left[LC \frac{\partial^2}{\partial t^2} - LG \frac{\partial}{\partial t} - \frac{\partial L / \partial x}{L} \frac{\partial}{\partial x} - \frac{\partial^2}{\partial x^2} \right] V \tag{18}$$

then equivalence #2 in (15) will also be fulfilled. Now the adjoint operator $\mathbf{L}^*$ that accomplishes (13) is found with its corresponding PDE (18) and initial and boundary conditions (16)-(17). The solution *V* of this PDE can only be different from zero if a non vanishing right side is assigned to $\mathbf{L}^* V$. Looking back to equation (11) one can equate

$$\mathbf{L}^* V = 2\delta(x - x_1)[U(x,t;\alpha) - \lambda(t)] \tag{19}$$

to continue the transformations of (11) and use the property of $\mathbf{L}^*$ being the adjoint operator to **L** according to the inner product (14).

$$
\begin{aligned}
&J(C+\delta C)-J(C)\\
&=\int_0^{2T}\int_{-\infty}^{\infty}\delta U\cdot\left(\mathbf{L}^* V\right)dx\,dt\\
&=\int_0^{2T}\int_{-\infty}^{\infty}\left(\mathbf{L}\,\delta U\right)\cdot V\,dx\,dt\\
&=\int_0^{2T}\int_{-\infty}^{\infty}V\left[L\delta C U_{tt}+LC\delta U_{tt}+LG\delta U_t+\frac{L_x}{L}\delta U_x-\delta U_{xx}\right]dx\,dt\\
&=\int_{-\infty}^{\infty}\delta C\int_0^{2T}VLU_{tt}dt\,dx\\
&\quad+\underbrace{\int_0^{2T}\int_{-\infty}^{\infty}V\left[LC\delta U_{tt}+LG\delta U_t+\frac{L_x}{L}\delta U_x-\delta U_{xx}\right]dxdt}_{\to 0\ for\ \|\delta C\|\to 0}
\end{aligned}
\tag{20}
$$

From (20) and (10) it follows that

$$
\nabla J(C)=\int_0^{2T}LV\frac{\partial^2}{\partial t^2}U dt=-\int_0^{2T}L\frac{\partial}{\partial t}V\frac{\partial}{\partial t}U dt. \tag{21}
$$

This gradient can be calculated by solving two IBVP: One forward problem for the direct wave (4)-(7) and one backward problem for the adjoint wave (16)-(19).

Double-sided reflection data

For the simultaneous reconstruction of *C(x)* and *G(x)* it is necessary to take two independent measurements. As shown in the previous section one choice will be the two reflection measurements from both sides of the sensor:

$$
\lambda_1(t)=U_a(x_1,t),\qquad \lambda_2(t)=U_e(x_2,t) \tag{22}
$$

It is also necessary to choose another cost function in order to minimize the error between the simulation and the measurements simultaneously. Choosing $J(\alpha)=J(C,G)$ as

$$
J(\alpha)=\sum_{i=1}^{2}\int_0^{2T}\left[U_i(x_i,t;\alpha)-\lambda_i(t)\right]^2 dt. \tag{23}
$$

The determination of the two gradients is very similar to the transformations above. It leads to the same adjoint PDE for $\mathbf{L}^*$ as in equation (18). But two different backward problems have to be calculated according to the two different forward solutions U_1 and U_2. The right sides of the adjoint problems are given by

$$
\mathbf{L}^* V_i=2\delta(x-x_i)\left[U_i(x,t;\alpha)-\lambda_i(t)\right],\ i=1,2 \tag{24}
$$

and the initial and boundary conditions have to be chosen to fulfil

$$V_i(x,2T)=0,\quad \frac{\partial}{\partial t}V_i(x,2T)=0,\quad -\infty<x<\infty,\, i=1,2, \tag{25}$$

$$V_i(-\infty,t)=0,\quad \frac{\partial}{\partial t}V_i(\infty,t)=0,\quad 0\le t\le 2T,\, i=1,2. \tag{26}$$

For each given $\alpha=(C(x),G(x))$ one can solve the forward problems for $U_1(x,t)$ and $U_2(x,t)$ and the backward problems for $V_1(x,t)$ and $V_2(x,t)$ and calculate the gradients of $J(\alpha)$ with respect to C and G, respectively:

$$\nabla^C J(\alpha)=-\sum_{i=1}^{2}\int_0^{2T} L\frac{\partial}{\partial t}V_i\frac{\partial}{\partial t}U_i\,dt \tag{27}$$

$$\nabla^G J(\alpha)=\sum_{i=1}^{2}\int_0^{2T} LV_i\frac{\partial}{\partial t}U_i\,dt \tag{28}$$

Reconstruction of the parameter distribution

To determine the distribution of $\alpha=C(x)$ a conjugate gradient (cg) method is appropriate if the gradient of the function to be minimized can be calculated explicitly and very easily. Starting with a parameter distribution $\alpha^{(0)}$ the first search direction is given by the direction of steepest decent $P^{(0)}=-\nabla J(\alpha^{(0)})$. The next parameter distribution can be calculated by

$$\alpha^{(k+1)}=\alpha^{(k)}+\gamma^{(k)}P^{(k)} \tag{29}$$

where $\gamma^{(k)}$ is the optimal step-size to minimize the cost function based on the former parameter distribution $\alpha^{(k)}$ and the search-direction $P^{(k)}$:

$$\gamma^{(k)}=\min_{\gamma} J\left(\alpha^{(k)}+\gamma\cdot P^{(k)}\right). \tag{30}$$

The main effort of computation in this minimization is due to the large number of cost function analysis. Therefore an effective numerical algorithm concerning minimum function calls is the core of a fast reconstruction algorithm. In comparison to conventional cg-methods the following search direction $P^{(k+1)}$ is not only the direction of steepest decent at $\alpha^{(k+1)}$ but also a combination of former search-directions.

$$P^{(k+1)}=-\nabla J\left(\alpha^{(k+1)}\right)+\frac{\left\|\nabla J\left(\alpha^{(k+1)}\right)\right\|_2^2}{\left\|\nabla J\left(\alpha^{(k)}\right)\right\|_2^2}\cdot P^{(k)} \tag{31}$$

This leads to a faster convergence and less calculation effort. The cg-method was chosen according to Fletcher and Reeves (1964[30]) – similar results were carried out by using the cg-method according to Polak and Ribière (1969[31]).
During simultaneous reconstruction of $C(x)$ and $G(x)$ the minimum search in (30) will be extended to a two-dimensional search:

$$\left(\gamma^{(k)},\eta^{(k)}\right)=\min_{\gamma,\eta} J\left(C^{(k)}+\gamma\cdot P_C^{(k)},G^{(k)}+\eta\cdot P_G^{(k)}\right) \tag{32}$$

Especially in this two-dimensional search the choice of an algorithm with as few function calls as possible is of crucial importance. The simplex method developed by Nelder and Mead (1965[32]) and the complex method by Box (1965[33]) lead to fast optimization algorithms even in the simultaneous reconstruction of two parameter functions. At one- and two-parameter optimization the conjugate gradient algorithm terminates if there is no significant change in the value of two consecutive cost functions. Figure 4 shows the flow chart of the preferred cg-method.

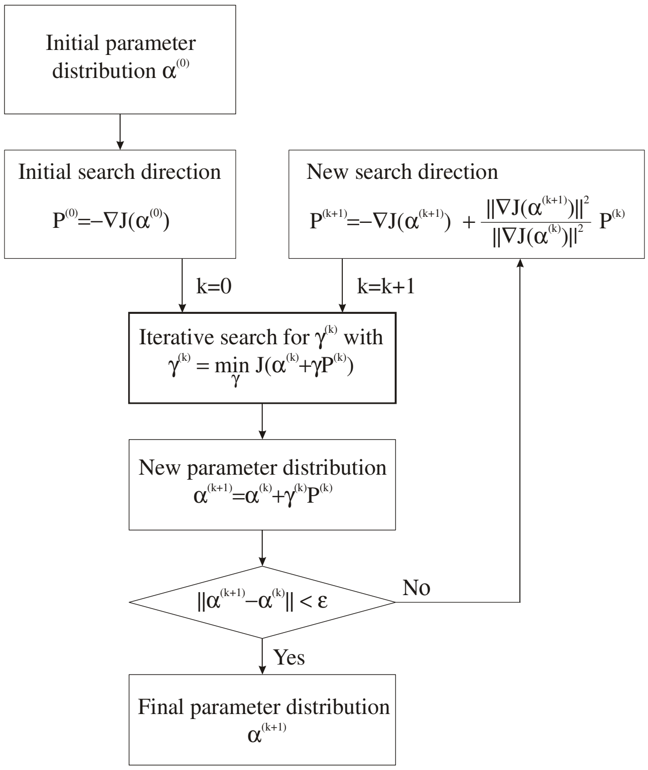

Fig. 4. Flow chart of the Fletcher-Reeves conjugate gradient method

When using two measurements which show only small differences in the reflected signal than the corresponding calculated parameter distribution shows only small variations as well.

Determination of the water content

The capacitance profile $C(x)$ describes the electrical properties of the whole medium around the conductors of the sensitive transmission-line. But strictly speaking, the capacitance at any point of the profile is not independent on the frequency. For simplification, we assume that there may be a constant value for C for the used TDR frequency range depending on feeding cable properties and length. If the sensor is not insulated $C(x)$ can be easily transformed into the relative permittivity of the medium $\varepsilon_m(x)=L_0c_0^2C(x)$, where L_0 specifies the inductance of the sensor and c_0 the speed of light in vacuum. If the sensor is insulated with some dielectric material the total capacitance $C(x)$ represents the combination of insulation and soil. Therefore a sensor specific transformation from C to the relative permittivity ε of the soil is necessary.

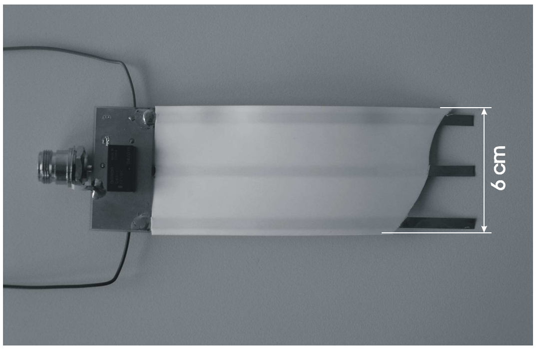

Fig. 5. Insulated flat-ribbon-cable (short section with bare conductors to visualize the geometry and the electrical connection of the cable) with a sensor switch between coaxial cable and flat-ribbon-cable

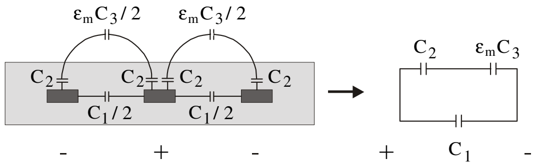

Fig. 6. Capacitance model of the insulated flat-ribbon-cable from Figure

The flat-ribbon-cable used for many applications of the SMG is shown in Figure 5. It has been developed and patented by the Institute of Meteorology and Climate Research at the Forschungszentrum Karlsruhe (Brandelik et al., 1998[34]). The cable consists of three flat copper wires covered with polyethylene. The electrical field is concentrated around the conductors and defines the sensitive area of 3 to 5 cm around the cable depending on the permittivity. The electric properties of the flat-ribbon-cable used in this work can be measured and calculated (cf. Figure 6 and table 1).

Table 1. Cable parameters for the sensor cable in Figure 5

Circuit Element	C_1 [pF/m]	C_2 [pF/m]	C_3 [pF/m]	L_0 [nH/m]
Measured Value	3.4	323	14.8	756
Calculate Value	4.0	308	13.7	785

According to the equivalent circuit of Figure 6 the total capacitance C can be expressed by three capacitances C_1, C_2, and $\varepsilon_m C_3$ and can be transformed into a direct relation between the relative permittivity ε_m of the surrounding soil and the total capacitance:

$$C(\varepsilon_m) = C_1 + \frac{C_2 \varepsilon_m C_3}{C_2 + \varepsilon_m C_3} \tag{33}$$

The three unknown capacitances C_1, C_2, and C_3 were derived from calibration measurements of three different materials with well known dielectric properties, e.g. air, oil, and water. The inductance was determined by measuring the wave impedance with a variable resistor at the end of the cable adjusted for minimum reflection. The values for the cable of Figure 5 are given below (Hübner, 1999[35]).

The permittivity of the soil can now be transformed to the volumetric water content by standard transformations for arbitrary soils (e.g. Topp et al., 1980[3]) or soil specific calibration functions determined from laboratory test series. The accuracy of the water content distribution depends highly on the accuracy of this transformation. The deviation due to insufficient knowledge of the material can easily exceed the errors of the reconstruction of the capacitance profile *C(x)*.

The total conductance $G(x)$ describes the conductivity of the material between the copper wires, i.e. the system of polyethylene insulation and the surrounding material. The determination of the water content distribution of the surrounding material does not require the knowledge of the conductivity distribution of the material, but it cannot be neglected during the reconstruction of $C(x)$.

Field results

The algorithm has been tested successfully on artificial data for one and two sided measurements (cf. Schlaeger, 2005[18]). In the following it is verified on field measured data. The results at the full-scale levee were carried out using measurements from both sides of the sensor cable, whereas the flood warning system was equipped with single sided rod-probes of 60 cm length.

Measuring of soil water on a full-scale levee model

In order to investigate transient hydraulic processes in levees during a flood, a full-scale levee model at the Federal Waterways and Research Institute was equipped with 12 flat band cables between 0.7 m and 3.0 m in length by the Institute of Soil Mechanics and Rock Mechanics, University of Karlsruhe. The model is built up homogeneously with uniform sand (grain size 0.2 to 2 mm) and it is based on a waterproof sealing of plastic. As a result of this construction, the water infiltrating into the levee will flow to a drain at the toe of the land side slope and directed to a measuring device (cf. Figure 7).

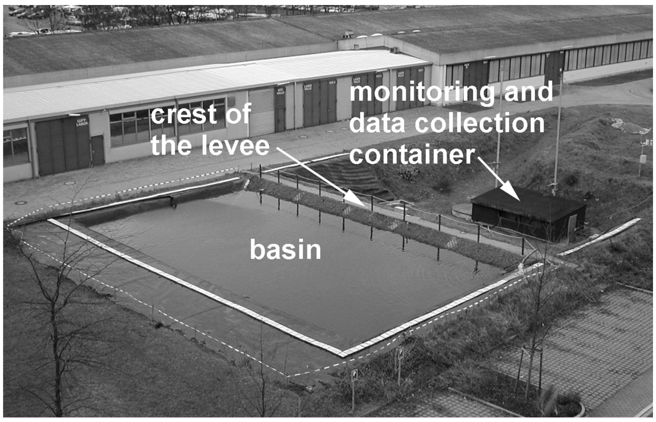

Fig. 7. Full-scale levee model at the Federal Waterways and Research Institute (BAW) in Karlsruhe during a flood simulation test in December 2000 (steady state of seepage condition)

In the course of the investigation mentioned above, flood simulation tests and sprinkling tests were carried out on the levee model (cf. Scheuermann and Brauns, 2002[37], Scheuermann et al. 2001[38]). Figure 8 shows the steady state of seepage condition during a flood simulation test in December 2000. The measurements of water content were reconstructed spatially along the cable and interpolated as distribution of saturation in the considered cross section. On the water side the water level in the basin is shown, and the position of the phreatic line within the body of the levee is given, as estimated from the pore water pressure measurements in the base of the levee. It can be seen that the measurements of the water content correspond very well with the position of the phreatic line. During the flood simulation tests on the levee model it was discovered that the percolation area below the phreatic line does not become fully saturated. Up to 15% of the pore space remained filled with air.

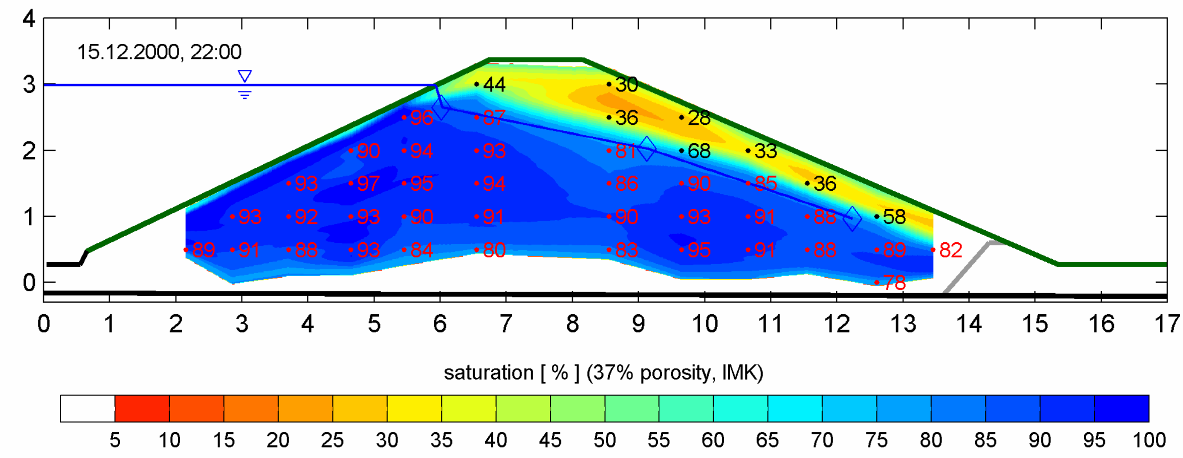

Fig. 8 Interpolated distribution of saturation in the levee model measured with the cable sensors during a flood simulation test in December 2000. The points represent the positions of the cable sensors, and the numbers next to the points show the measured values. The phreatic line was derived from the piezometer measurements in the base of the model

With this system it is possible to record the distribution of water content in a cross section within 5 minutes. This way, measurements of the water content with a spatial resolution of 3 cm are possible. The profiles of saturation can be determined with an average deviation of ± 4% compared to other independent measurements. With this technique the observation of transient hydraulic processes within a levee was made possible with this spatial resolution. However, it takes several hours on a common desktop PC to reconstruct the measuring signals in a water content profile for a cross section. This means that with this reconstruction algorithm real time monitoring is not possible at the moment. But direct evaluation of the measured signals can lead to an improvement by means of localization of water content anomalies.

Soil Moisture Measurements for a Flood Warning System

Flood peaks in small or middle size catchment areas are primarily formed by the fast runoff components. These temporal high dynamic components take place in the upper part of the soil horizon. The state of these components can be indicated by distributed soil moisture measurements (see figure 9).

With only slight disturbance of the occurring pseudogleyed cambisol 46 vertical twin rod probes were established in the Goldersbach catchment area (Tübingen, Germany). The temporal resolution of these measurements is 3 hours.

These mesoscale measurements are regionalised to the catchment area scale by processing of scenes of the remote sensor Landsat-TM 6. A principal component analysis transforms the 6 Landsat bands into 4 principal components. The classification of the components to brightness, greenness and wetness (soil moisture) is achieved by their factor loadings. The dynamic range of soil moisture is registered by the comparison of different Landsat scenes.

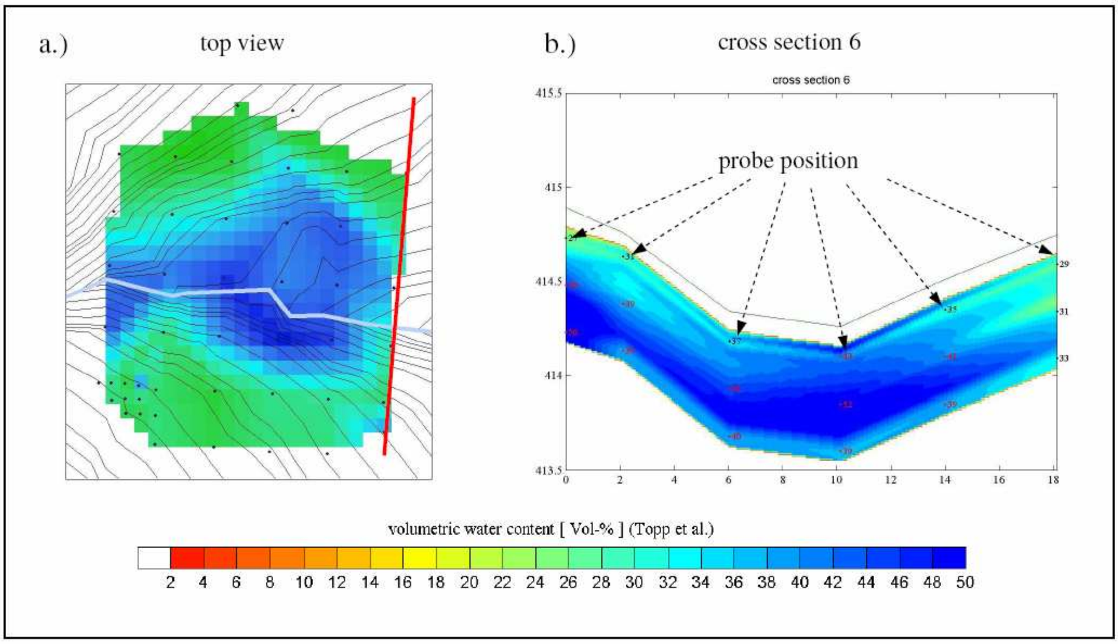

Fig. 9. Measured and interpolated saturation distribution of the soil moisture measurement cluster as a.) top view and b.) cross section. The top view shows twin rod probes as points, contour lines and brook course. In the cross section measurement values are displayed explicit in the heights of 10, 30 and 55 cm

Conclusions

A fast inversion technique is presented that derives capacitance profiles in high spatial resolution from single TDR reflection measurements. The algorithm is based on an optimization approach to minimize the difference between the measurement and simulated TDR reflection data depending on a given parameter distribution. The optimization is done with conjugate gradients due to the fact that the gradient can be calculated explicitly. This gradient can be determined very fast by solving only two initial-boundary-value-problems instead of several hundred when using standard Hessian matrix inversion techniques. The algorithm iterates very fast and leads to reliable soil moisture profiles which can be derived from the capacitance profiles by standard transformations.

The results of this study of this new inversion technique for time domain reflectometry data show that single-sided reflection data are capable for the reconstruction of the soil moisture profile for lossless (or low-loss) soils. The full information content of one single travel-time roundtrip can be used to determine the capacitance profile $C(x)$ and the associated volumetric water content on a standard PC in reasonable time. In the case of lossy soils more information is required. The knowledge of the conductance profile $G(x)$ or an experimental determined relationship between capacitance and conductance for the used sensor and soil can improve the determination of moisture profiles using only one single measurement. If none of this knowledge is available one more independent reflection measurement is required.

The presented inversion technique is also suitable for the simultaneous reconstruction of capacitance and conductance profile using double-sided reflection data. The resulting profiles are more reliable than single-sided reconstructions with standard assumptions to the conductivity (e.g. constant conductivity distributions). The simultaneous reconstruction of $C(x)$ and $G(x)$ and the associated volumetric water content can also be done within a reasonable time.

References

[1] Robinson, D.A., Jones, S.B., Wraith, J.M., Or, D., and S.P. Friedman: A review of advances in dielectric and electrical conductivity measurement in soils using time domain reflectometry, Vadose Zone Journal, 2, 444-475, 2003.

[2] Birchak, J.R., Gardner, C.G., Hipp, M.E., and J.M. Victor,: High dielectric constant microwave probes for sensing soil moisture, Proceedings of the IEEE, 62, 93-98, 1974.

[3] Topp, G. C., J. L. Davis, and A. P. Annan, Electromagnetic determination of soil water content. Measurements in coaxial transmission lines, Water Resources Research, 16(3), 574-582, 1980.

[4] Topp, G.C., Davis, J.L., and A.P. Annan: Electromagnetic determination of soil water content using TDR: I Applications to wetting fronts and steep gradients, Soil Sci. Soc. Am. J., 46, 672-678, 1982.

[5] Topp, G.C., Davis, J.L., and A.P. Annan: Electromagnetic determination of soil water content using TDR: II Evaluation of installation and configuration of parallel transmission lines , Soil Sci. Soc. Am. J., 46, 678-684, 1982.

[6] Topp, G.C., and J.L. Davis: Measurement of soil water content using time-domain reflectometry (TDR): A field evaluation, Soil Sci. Soc. Am. J., 49, 19-24, 1985.

[7] Dasberg, S., and F.N. Dalton: Time domain reflectometry field measurements of soil water content and electrical conductivity, Soil Sci. Soc. Am. J., 49, 293-297, 1985.

[8] Heimovaara, T. J., and W. Bouten, A computer-controlled 36-channel time domain reflectometry system for monitoring soil water content, Water Resources Research, 26, 2311-2316, 1990.

[9] Hook, W.R., Livingston, N.J., Sun, Z.J., and P.B. Hook: Remote diode shorting improves measurement of soil water by time domain reflectometry, Soil Sci. Soc. Am. J., 56, 1384-1391, 1992.

[10] Feng, W., Lin, C.P., Deschamps, R.J. and V.P. Drnevic: Theoretical model of a multisection time domain reflectometry measurement system, Water Resources Research, 35, 8, 2321-2331, 1999.

[11] Pereira, D.S.: Développement d'une nouvelle méthode de détermination des profils de teneur en eau dans les sols par inversion d'un signal TDR, Ph.D. thesis, Lab. D'Etude des Transf. En Hydrol. Et Environ., (LTHE), Univ. Joseph Fourier-Grenoble I, Grenoble, France, 1997.

[12] Todoroff, P., Lorion, R., and J.D. Lan Sun Luk: L'utilisation des algorithmes génétiques pour l'identification de profil hydriques de sol a partir de courbes réflectrométriques, C.R. Acad. Sci. Ser. IIa, Sci. Terre Planetes, 327, 607-610, 1998.

[13] Oswald, B.: Full wave solution of inverse electromagnetic problems, Ph.D. thesis Swiss Federal Institute of Technology, Zürich 2000.

[14] Heimovaara, T.J., Huismann, J.A., Vrugt, J.A., and W. Bouten: Obtaining the spatial distribution of water content along a TDR probe using the SCEM-UA Bayesian inverse modelling scheme, Vadose Zone Journal, 3, 1128-1145, 2004.

[15] Lundstedt, J., and S. He, A time-domain optimization technique for the simultaneous reconstruction of the characteristic impedance, resistance and conductance of a transmission line, J. Electromagn. Waves and Appl., 10(4), 581-602, 1996.

[16] Norgren, M., and S. He, An Optimization approach for the frequency-domain inverse problem for a nonuniform LCRG transmission line, IEEE Transaction on Microwave Theory and Technique, 44(8), 1503-1507, 1996.

[17] Schlaeger, S.: Inversion von TDR-Messungen zur Rekonstruktion räumlich verteilter bodenphysikalischer Parameter, Ph.D. thesis, 189 pp., Veröffentlichungen des Institutes für Bodenmechanik und Felsmechanik der Universität Fridericiana in Karlsruhe, vol. 156, Karlsruhe, Germany, 2002.

[18] Schlaeger, S.: A fast TDR-inversion technique for the reconstruction of spatial soil moisture content. Hydrology and Earth System Sciences, 9, 481-492, 2005.

[19] Scheuermann, A., S. Schlaeger, C. Hübner, A. Brandelik, and J. Brauns, Monitoring of the spatial soil water distribution on a full-scale dike model, in Proceedings of the Fourth International Conference on Electromagnetic Wave Interaction with Water and Moist Substances, Weimar, MFPA, 343-350, 2001.

[20] Becker, R., A. Brandelik, C. Hübner, W. Schädel, A. Scheuermann, and S. Schlaeger, Soil and snow moisture measurement system with subsurface transmission lines for remote sensing and environmental applications – Results of the Soil Moisture Group of the University of Karlsruhe, in Proceedings of the Open Symposium on Propagation and Remote Sensing, URSI Commission-F, Garmisch-Partenkirchen, Germany, February 12-14, 2002.

[21] Stacheder, M., C. Hübner, S. Schlaeger, and A. Brandelik, Combined TDR and low frequency permittivity measurements for continuous snow wetness and snow density determination, in Electromagnetic Aquametry, K. Kupfer (ed.), Springer, Berlin, Heidelberg, New York, 2005.

[22] Becker, R., A. Bieberstein, C. Hübner, R. Nüesch, W. Schädel, A. Scheuermann, S. Schlaeger, and R. Schuhmann, Nondestructive in situ and online measurements of soilphysical parameters, in Soil and Rock America 2003, 12th Panamerican Conference on Soil Mechanics and Geotechnical Engineering, 39th U.S. Rock Mechanics Symposium, Cambridge , June 22-26, 2003.

[23] Engquist, B., and A. Majda, Absorbing boundary conditions for the numerical simulation of waves, Mathematics of Computation, 31, 629-651, 1997.

[24] Becker, R., and C. Hübner, Messgeräteentwicklungen der Soil Moisture Group, in Kolloquium mit Workshop "Innovative Feuchtemessung in Forschung und Praxis", Karlsruhe, Germany, July 3-4, 2003.

[25] Becker, R.: Spatial time domain reflectometry for monitoring transient soil moisture profiles, Ph.D. thesis, Institut für Wasser und Gewässerentwicklung – Bereich Wasserwirtschaft und Kulturtechnik, Mitteilungen Heft 228, Universität Karlsruhe, 2004.

[26] Becker, R., and S. Schlaeger: Spatial time domain reflectometry with rod probes, Proceedings of the 6th Conference on “Electromagnetic Wave Interaction with Water and Moist Substances”, ISEMA 2005, Weimar, Germany, May 29 – June 1, 2005.

[27] He, S., S. I. Kabanikhin, V. G. Romanov, and S. Ström, Analysis of the Green’s function approach to one-dimensional inverse problems. Part I: One parameter reconstruction, J. Math. Phys., 34(12), 5724-5746, 1993.

[28] Håkansson, G: Reconstruction of soil moisture profile using time-domain reflectometer measurements, Master thesis, Royal Institute of Technology, Department of Electromagnetic Theory, Stockholm, 1997.

[29] He, S., V. G. Romanov, and S. Ström, Analysis of the Green's function approach to one-dimensional inverse problems. Part II: Simultaneous reconstruction of two parameters, J. Math. Phys., 35(5), 2315-2335, 1994.

[30] Fletcher, R., and C. M. Reeves, Function minimization by conjugate gradients, The Computer Journal, 7(2), 149-154, 1964.

[31] Polak, E., and G. Ribière, Note sur la convergence de methodes de directions conjugees, Revue Française d'Informatique et de Recherche Operationelle, Serie Rouge, 3(16), 35-43, 1969.

[32] Nelder, J. A., and R. Mead, A simplex method for function minimization, The Computer Journal, 7(4), 308-313, 1965.

[33] Box, M. J.: A new method of constraint optimization and a comparison with other methods, The Computer Journal, 8(1), 43-52, 1965.

[34] Brandelik, A., C. Huebner, and R. Schuhmann, Moisture sensor for large area layers (German patent no. 4432687, European patent no. 0804724, US patent no. 5942904), June 16,1998.

[35] Hübner, C, Entwicklung hochfrequenter Messverfahren zur Boden- und Schneefeuchtebestimmung, Ph.D. thesis, 199 pp., Forschungszentrum Karlsruhe, Institute for Meteorology and Climate Research, Scientific Report FZKA 6329, Karlsruhe, 1999.

[36] Hübner, C., S. Schlaeger, R. Becker, A. Scheuermann, A. Brandelik, W. Schädel, and R. Schuhmann, Advanced measurement methods in time domain reflectometry for soil moisture determination, in Electromagnetic Aquametry, K. Kupfer (ed.), Springer, Berlin, Heidelberg, New York, 2005.

[37] Scheuermann, A., Brauns, J. Die Durchfeuchtung von Deichen – Modellversuche und Analyse, In: DGGT 12. Donau-Europäische-Konferenz 2002, Proceedings, Passau, 197-200, 2002.

[38] Scheuermann, A., Schlaeger, S., Hübner, C., Brandelik, A., Brauns, J. Monitoring of the spatial soil water distribution on a full-scale dike model, In Kupfer, K. and C. Hübner: Fourth International Conference on Electromagnetic Wave Interaction with Water and Moist Substances, Weimar, Germany, May 13-16, S. 343-350, 2001.

Information on the authors

Dr.-Ing. *Stefan Schlaeger* studied techno-mathematics at Karlsruhe University. In 2002 he completed his doctor's degree at the Faculty of Civil Engineering at Karlsruhe on the subject of moisture measurement with TDR. He is a member of the Soil Moisture Group and since 2005 has been working as a self-employed engineer.
Contact: SCHLAEGER mathematical solutions & engineering, Lammbergweg 23, 32805 Horn-Bad Meinberg, Germany. Phone +49 (5234) 2046-31, Fax +49 (5234) 2046-35, E-Mail : stefan.schlaeger@smg.uka.de

Dr.-Ing. *Rolf Becker* studied Physics at the University of Bonn. He worked as research assistant in Hydrology at the University of Karlsruhe and is co-founder of the Soil Moisture Group. He received his doctoral degree in 2004 for his dissertation about infiltration monitoring with profiling time domain reflectometry techniques. Today Rolf Becker is head of development at IMKO Micromodultechnik GmbH.

Dr.-Ing. *Wolfram Schädel* studied civil engineering, continued and completed his doctor's degree at the Faculty of Civil Engineering at Karlsruhe in 2006. The subject of his thesis was the implication of online moisture measurements for an improved flood-warning-system. He is member of the Soil Moisture Group and since 2006 has been working as a self-employed engineer.

Dr.-Ing. *Alexander Scheuermann* studied civil engineering at the University of Karlsruhe. From 1998 until 2001 he visited the post-graduate programme "Natural Disasters". 2005 he completed his doctor's degree at the Faculty of Civil Engineering, Geo- and Environmental Sciences at Karlsruhe on the subject of transient seepage through quasi-homogeneous dykes. He is a member of the Soil Moisture Group and he works as a senior researcher at the Institute of Soil Mechanics and Rock Mechanics of the University of Karlsruhe.

Dipl.-Ing. *Holger Wörsching* completed his studies in civil engineering at the University of Karlsruhe in 2003. Since then he has been working as a graduate research assistant at the Institute of Soil Mechanics and Rock Mechanics at the University of Karlsruhe (TU), Germany on the subject of dam stability and flood prevention. He is a member of the Soil Moisture Group of the University of Karlsruhe, which deals with various geophysical moisture measurement methods.